Saudi Journal of Biological Sciences xxx (2017) xxx–xxx

Contents lists available at ScienceDirect

Saudi Journal of Biological Sciences

journal homepage: www.sciencedirect.com

Original article

# A calcium channel blocker nifedipine distorts the effects of nano-zinc oxide on metal metabolism in the marsh frog *Pelophylax ridibundus*

Halina Falfushynska [a,*], Lesya Gnatyshyna [a,b], Oksana Horyn [a], Arkadii Shulgai [b], Oksana Stoliar [a]

[a] *Research Laboratory of Comparative Biochemistry and Molecular Biology, Ternopil National Pedagogical University, Kryvonosa Str. 2, 46027 Ternopil, Ukraine*
[b] *I.Ya. Horbachevsky Ternopil State Medical University, Maidan Voli 1, 46001 Ternopil, Ukraine*

ARTICLE INFO

*Article history:*
Received 7 May 2017
Revised 1 October 2017
Accepted 2 October 2017
Available online xxxx

*Keywords:*
Marsh frog
Nano-ZnO
Nifedipine
Metallothionein
Vitellogenin
Stress response

ABSTRACT

Global decline of amphibian populations causes particular concern about their vulnerability to novel environmental pollutants, including engineering nanomaterials and pharmaceutical products. We evaluated the bioavailability of nanoform of zinc oxide (n-ZnO) in frog *Pelophylax ridibundus* and determined whether co-exposure to a common pharmaceutical, a calcium-channel blocker nifedipine (Nfd) can affect this bioavailability. Male frogs were exposed for 14 days to the tap water (Control) and n-ZnO (3.1 μM), $Zn^{2+}$ (3.1 μM, as a positive control for n-ZnO exposures), Nfd (10 μM), and combination of n-ZnO and Nfd (n-ZnO + Nfd) in environmentally-relevant concentration. Exposure to $Zn^{2+}$ or n-ZnO led to up-regulation of metal-binding proteins, metallothioneins (MTs) in the liver and Zn-carrying vitellogenin-like proteins in the blood plasma. Notably, upregulation of MTs by $Zn^{2+}$ or n-ZnO exposures combined with increased binding of Zn and Cu to MTs. This was associated with the more reducing conditions in the liver tissue indicated by elevated lactate to pyruvate ratio. Nfd suppressed the binding of Zn and Cu to MTs and led to a decrease in Lactate/Pyruvate ratio and elevated protein carbonylation indicating pro-oxidant conditions. Redox status parameters were not directly related to DNA fragmentation, nuclear abnormalities or suppression of cholinesterase activity indicating that factors other than oxidative stress are involved in cytotoxicity of different pollutants and their combinations. Furthermore, activity of Phase I biotransformation enzyme (CYP450 oxidase measured as EROD) was elevated in Nfd-containing exposures and in $Zn^{2+}$ exposed frogs. Tyrosinase-like activity in the frog liver was strongly stimulated by $Zn^{2+}$ but suppressed by n-ZnO, Nfd and n-ZnO + Nfd. These findings show that Nfd modulates homeostasis of essential metals in amphibians and emphasize that physiological consequences of combined n-ZnO and Nfd exposures are difficult to predict based on the mechanisms of single stressors.


## 1. Introduction

Freshwater organisms including amphibians are increasingly exposed to complex mixtures of environmental pollutants including novel chemicals such as nanomaterials and pharmaceuticals. According to a recent inventory, more than 1600 consumer products containing nanomaterials were on the market in 2013 (Nanotech-Project, 2013, Vance et al., 2015). Zinc oxide nanoparticles (n-ZnO) are commonly used in a broad range of consumer products including sunscreens baby powders, antifungal creams, anti-dandruff shampoos, and fabric treatments for UV protection (Osmond and McCall, 2010, Adamcakova-Dodd et al., 2014; Sirelkhatim et al., 2015). n-ZnO from consumer goods can leach into the environment raising concerns about the potential toxicity of n-ZnO to aquatic organisms. Adverse effects of n-ZnO have been shown in mollusks, fish and amphibians (Vandebriel and De Jong, 2012, Falfushynska et al., 2015b, Pandurangan and Kim, 2015, Kim et al., 2017). However, the molecular mechanisms of these effects are not fully understood. Oxidative stress is commonly invoked as a potential mechanism of n-ZnO toxicity (Liu et al., 2016). Recent studies in showed that n-ZnO also affects proteolytic pathways, apoptosis and thyroid hormone synthesis in amphibians (Falfushynska et al., 2017) and metallothioneins expression, oxidative stress response and lysosomal membrane permeability in mollusks (Falfushynska et al., 2015a). Notably, toxic effects of n-ZnO

* Corresponding author.
*E-mail addresses:* halynka.f@gmail.com, falfushynska@tnpu.edu.ua (H. Falfushynska).
Peer review under responsibility of King Saud University.

Production and hosting by Elsevier

https://doi.org/10.1016/j.sjbs.2017.10.004
1319-562X/

Please cite this article in press as: Falfushynska, H., et al. A calcium channel blocker nifedipine distorts the effects of nano-zinc oxide on metal metabolism in the marsh frog *Pelophylax ridibundus*. Saudi Journal of Biological Sciences (2017), https://doi.org/10.1016/j.sjbs.2017.10.004

are often weaker than those of free $Zn^{2+}$ indicating that metal from n-ZnO particles may not be readily bioavailable (Falfushynska et al., 2015b, Falfushynska et al., 2017).

Nanomaterials in freshwater environments commonly co-occur with other chemical stressors such as pharmaceuticals and personal care products (PPCPs) (Buzea et al., 2007, Daughton, 2016). Ecotoxicological effects of PPCPs are likewise poorly understood, although their high biological activity in target species (such as humans or domestic animals) creates potential for similar effects in aquatic organisms. In this study, we focused on a common calcium influx inhibitor nifedipine (Nfd), which is widely used as an antianginal and antihypertensive medicine and is on the World Health Organization (WHO) Model List of Essential Medicines (WHO, 2015). Despite its partial microbial and photocatalytic breakdown in the environment, Nfd and its degradation products (nitroso-, nitro-, azoxy- and N,N′-dioxide-derivatives) are common pollutants in municipal sewage effluents and in surface waters (Hayase et al., 1995). Our earlier study showed that n-ZnO toxicity in bivalve mollusks is modulated by Nfd causing increase in the DNA fragmentation (Falfushynska et al., 2015a). In amphibians, Ndf exposure caused oxidative stress indicated by elevated production of reactive oxygen species, accumulation of lipid peroxidation products and oxidized glutathione (Falfushynska et al., 2017).

Understanding ecotoxicological effects of multiple pollutant exposures in amphibians has become a focus of attention due to global amphibian population declines (Johnson et al., 2016, Prokić et al., 2017). Frogs are sensitive to a range of environmental pollutants due to their semi-permeable skin especially during the aquatic life cycle stages, and exposures to sublethal concentrations of environmental pollutants may be complicit factors in deteriorating amphibian health (Kloas and Lutz, 2006). The ecotoxicity of nanoparticles and PPCPs in frogs has not been extensively studied (Nations et al., 2011). Our recent study in *Pelophylax ridibundus*, a common European marsh frog, showed that Nfd may act as a pro-oxidant and endocrine disruptor in this species (Falfushynska et al., 2017). Nfd also increased the cellular thiol content due to elevated levels of the thermostable thiol-containing proteins (putative MTs) and glutathione (Falfushynska et al., 2017). Based on these findings, we hypothesized that Nfd can affect homeostasis of essential metals with high affinity to thiol groups (such as $Zn^{2+}$ and $Cu^{2+}$) increasing metal toxicity in frogs and inducing genotoxicity, which is a common consequence of disrupted metal homeostasis (Mulware, 2013). To test this hypothesis, we measured $Zn^{2+}$ and $Cu^{2+}$ binding to MTs and Zn-containing vitellogenin-like proteins in frogs exposed to n-ZnO, Nfd and their combinations, assessed parameters of genotoxicity (DNA fragmentation and nuclear abnormalities). We also determined the changes in cellular redox status (by measuring the ratio of lactate to pyruvate reflective of the NADH/$NAD^+$ ratio (Sun et al., 2012) and assessing the levels of carbonylated proteins) to determine whether changes in the $Zn^{2+}$ and $Cu^{2+}$ binding are associated with the cellular redox shifts. Activity of CYP450 monooxygenase (measured as EROD activity) was determined to assess activation of detoxification pathways by n-ZnO and Nfd exposures, and activities of metal-sensitive enzymes (including tyrosinase and cholinesterase (Frasco et al., 2005, Han et al., 2007, Pohanka, 2014) was measured to test the potential effects of disrupted $Zn^{2+}$ and $Cu^{2+}$ metabolism for cellular processes.

## 2. Materials and methods

### 2.1. Materials

Suspensions of n-ZnO (mean particle size 35 nm), reduced glutathione (GSH), bovine serum albumin, phenylmethylsulfonyl fluoride (PMSF), 5,5′-dithio-bis(2-nitrobenzoic acid) (DTNB), nicotinamide adenine dinucleotides (NADH, NAD, NADPH), EDTA, dihydrorhodamine, Hoescht 33342 dye, 2,4-Dinitrophenylhydrazine, tyrosin, hemoglobin, chymotrypsinogen, cytohrome *c*, myoglobin, ubiquitin, Sephadex G-50, β-mercaptoethanol, ethoxyresorufin, certified reference material ERM-BB422 and *Lactobacillus leichmannii* D-Lactate dehydrogenase were purchased from Sigma Chem. Co. (St. Louis, USA). All other chemicals were obtained from the Synbias (Kyiv, Ukraine), Bayer (Kyiv, Ukraine) and Balkanpharma-Dupnitsa (Dupnitsa, Bulgaria) commercial suppliers. All reagents were of the analytical grade or higher.

### 2.2. Animal maintenance and experimental exposures

A total of 60 replicates of adult males of *Pelophylax ridibundus* (*Rana ridibunda*) (8–10 cm long) were collected in September 2013, outside the breeding season of the local population of *P. ridibundus,* from a country site in the upstream portion of river Seret (near the village Ivachiv, 49°49′N, 25°23′E) where no industrial contamination could be detected. Frogs were transported to the laboratory in 60 L cages with aerated native water (dissolved oxygen concentration was 8.67 ± 0.51 mg·$L^{-1}$). Experiments were carried out in accordance with the national and institutional guidelines for the animal protection and welfare with permission of the Ministry of Ecology and Natural Resources of Ukraine, No 466/17.04.2013 and approval of the Committee on the Bio-Ethics at Ternopil National Pedagogical University (No 2/10.06.2013).

The *P. ridibundus* specimens in the trial, exposure conditions and experimental design of the study were the same as described in our earlier published work (Falfushynska et al., 2017). Briefly, frogs were acclimated in aerated, softened tap water (total hardness was 1.1 ± 0.07 mmol $L^{-1}$) and fed throughout the experiment with commercial "Turtle menu" (21% of protein, Aquarius, Ukraine). After seven days of preliminary acclimation, frogs were randomly distributed into five groups (10 individuals per group). One group was exposed to the fresh tap water only and was considered as a control (C). Four other experimental groups were exposed to the following compounds: (1) zinc nanooxide (n-ZnO), (2) dissolved zinc ($Zn^{2+}$ added as $ZnSO_4$, used as a positive control), (3) a potent vasodilator agent, dihydropyridine Calcium Channel Blocker nifedipine (dimethyl 2,6-dimethyl-4-(2-nitrophenyl)-1,4-dihydropyridine-3,5-dicarboxylate) (Nfd, 10 μM), and 4) a combination of n-ZnO with 10 μM Nfd (n-ZnO + Nfd). The concentrations of n-ZnO and $ZnSO_4$ were adjusted to correspond to the nominal concentration of 3.1 μM Zn in suspension and/or solution. The concentrations of the nanoparticles, free $Zn^{2+}$ and Nfd chosen for this study were within the range of concentrations range found in the field (for $Zn^{2+}$ and n-ZnO) and/or reflected the lowest observed effect concentrations (LOEC) (for Nfd). For n-ZnO approximately 95% of rivers in the EU would be predicted to amount 500 ng $L^{-1}$ or less (~6 nM n-ZnO) (NanoFATE 2010–2014). Concentration of Zn in the water at the sampling site was 20.2 ± 2.7 μg $L^{-1}$ ($n$ = 3). The concentrations used in this study (3.1 μM Zn) were well below this level.

All exposures were carried out for 14 days at 18 °C in 60 L tanks with aerated, softened tap water (10 animals per tank). There was no mortality of frogs during the acclimation or experimental exposures. After 14 days of exposure, the frogs were anesthetized by clove oil, the heparinized blood was collected from the heart, and plasma was separated immediately by centrifugation at 2000*g* for 10 min. The frogs were killed by a blow to the head, the spinal cord severed, and liver was removed immediately for experiments. Isolated livers of 8 frogs per each experimental group were perfused on ice. The circulating blood was drained using a 24-gauge needle (Yuria-Farm, Ukraine) attached to a syringe was inserted

Please cite this article in press as: Falfushynska, H., et al. A calcium channel blocker nifedipine distorts the effects of nano-zinc oxide on metal metabolism in the marsh frog *Pelophylax ridibundus*. Saudi Journal of Biological Sciences (2017), https://doi.org/10.1016/j.sjbs.2017.10.004

into the lumen of the liver with 8 ml of the saline/Ringer's solution (NaCl, 6.5 g, KCl, 0.14 g, $CaCl_2$, 0.03 g, $NaHCO_3$, 0.2 g, Glucose, 2.0 g, Distilled Water, 1000 ml), then livers were shock frozen and stored at −20 °C until further analyses. Plasma samples were obtained as the supernatants of heparinized (Biolik, Ukraine), anti-coagulated blood and immediately used for vitellogenin-like protein determination. For metal analysis in metallothioneins (MTs) samples were isolated from liver tissues and kept at −20 °C until metals assessed.

Analysis of the results of studying water parameters and thermostable proteins was carried out in triplicate, and all other measurements were carried out in 8 frog specimens.

### 2.3. Metal-binding proteins and metal content

Metallothioneins (MTs) were isolated from liver tissues of frogs as a thermostable protein fraction using size-exclusion chromatography on Sephadex G-50 as described elsewhere (Falfushynska and Stoliar, 2009). Briefly, 5% homogenate (w/v) of the liver tissue was prepared in ice-cold isolation buffer (10 mM Tris-HCl, pH 8.0) containing 10 mM 2-mercaptoethanol (to maintain the reducing conditions and avoid oxidation of MTs) and 0.1 mM PMSF (to inhibit proteolysis). Fractions of the chromatographic peak with high absorbance at 254 nm and a relatively high $D_{254}/D_{280}$ density ratios were identified as MTs-containing peaks (Kagi and Schaffer, 1988), pooled to obtain a total of 10 mL and applied to determine the content of metals (Cu and Zn).

Concentrations of metals (Cu and Zn) were determined in the liver tissue of the frogs and in the MT fraction of liver proteins. For this, fresh liver tissues (250 mg) or the pooled eluate of MTs fraction (10 mL) were digested in 5 mL metal-grade $HNO_3$ (LLC Merck, Moscow, Russian Federation) for 3 h at 105 °C in an air-tight acid-cleaned Teflon bomb. Concentrations of Zn and Cu was analyzed by the atomic absorption spectrometer with a flame detector (C-115, LOMO, St. Petersburg, Russian Federation). The detection limits for metals were 0.1 $\mu g \cdot g^{-1}$ wet mass for the tissue and MT fraction. The reliability of the metals measurements was assessed by analyzing ERM-BB422 fish muscle matrix certified reference material with known mass fractions of eight elements, among them zinc and copper; metal recovery was between 90% and 110%. Quality control was assessed by method of Standard Addition (Beukelman and Lord, 1960). Metal concentration in the MTs was presented as $\mu g \cdot g^{-1}$ wet mass (WM).

MTs content in the hepatic thermostable protein fraction was measured with MT-specific antibodies using a semi-quantitative biomarker enzyme-linked immunosorbent (ELISA) assay (M04406201-100, Biosence, Sweden) as described previously (Falfushynska et al., 2015a). Primary rabbit polyclonal antibody against cod MT and secondary antibody conjugated with Horseradish Peroxidase were added to each microplate successively and incubated. The absorbance was measured at 492 nm in an ELISA reader (Awareness Technology Stat-Fax-303 + Microstrip Reader, Palm City, FL, USA).

Vitellogenin-like proteins (Vtg-LP) were evaluated as the alkali-labile phosphate level, according to the method described by Nagler et al. (1987). It is based on the principle that trichloroacetic acid- precipitated phosphoproteins are subjected to an alkali treatment in order to release labile phosphates. The content of free phosphates was defined by the phosphomolybdenum assay.

### 2.4. Biomarkers of redox status and cellular stress

Liver tissue was homogenized (1:10 w:v) in ice-cold phosphate buffer (0.1 M, pH 7.4) containing 100 mM KCl, 1 mM EDTA and 0.1 mM PMSF with 12–15 strokes of a motor-driven Teflon Potter–Elvehjem homogenizer. The homogenate was centrifuged at 6000*g* for 10 min at 4 °C, and supernatants used for biomarker analysis. Concentrations of metabolites and enzyme activities (described in Sections 2.4.1–2.4.3) were standardized to the protein content of the homogenates. Protein concentrations were measured by the method of Lowry et al. (1951) using bovine serum albumin as a standard. The absorbance values were measured on the UV/Vis spectrophotometer LOMO-56 (LOMO, St. Petersburg, Russian Federation), and the extinction/emission values were measured on the f-max fluorescence microplate reader (Molecular Devices, Sunnyvale, CA, USA).

#### 2.4.1. Oxidative lesions and redox status

Protein carbonyl (PC) content was measured in the supernatant using the reaction of carbonyls with 2,4-Dinitrophenylhydrazine (DNPH) or HCl as a negative control (Reznick and Packer, 1994). After incubation with DNPH, proteins were precipitated by 100% thrichloroacetic acid and centrifuged at 12,000*g* for 10 min. The pellet was collected, washed with ethanol ethylacetate and dissolved in 8 M urea. The differences in absorbance between the DNPH- and the HCl-treated samples were determined spectrophotometrically at 375 nm, and the amount of carbonyl was determined by using a molar extinction coefficient of $2.2 \cdot 10^4$ $M^{-1} \cdot cm^{-1}$. Data were expressed as $\mu mole\ g^{-1}$ wet mass.

Tissue redox status was assessed using the lactate/pyruvate ratio. Lactate and pyruvate were assayed with standard spectrophotometric methods using bacterial D-Lactate Dehydrogenase (EC 1.1.1.28) from *Lactobacillus leichmannii* (D-LDH) as a coupling enzyme. Lactate concentrations were measured following the NAD-dependent enzymatic oxidation of lactate to pyruvate by D-LDH (Gawehn, 1988). Pyruvate was measured following the D-LDH-dependent conversion of pyruvic acid to D-lactic acid in the presence of NADH. Differences in the absorbance at 340 nm (reflecting a change in NADH concentration) measured before the start and 60 min after the start of the reactions were used to calculate lactate or pyruvate concentrations of the samples using the milimolar extinction coefficient for NADH of $\varepsilon_M = 6.22 \cdot mM^{-1} \cdot cm^{-1}$ (Lamprecht and Heinz, 1988).

#### 2.4.2. Genotoxicity markers

To assay the genotoxicity of exposures, levels of protein-free DNA strand breaks in liver tissue cells were determined by the alkaline DNA precipitation assay (Olive, 1988) based on using Hoescht 33342 dye in the presence of 0.4 M NaCl, 4 mM sodium cholate, and 0.1 M Tris (pH 9) (Bester et al., 1994). The amount of protein-free DNA strand breaks was related to the level of the protein in sample.

Genotoxic effect of model exposures was assessed in the erythrocytes by the frequency of the micronucleated erythrocytes (MN) (Baršienė et al., 2006), as well as erythrocytes with lobed nuclei (L), dumbbell-shaped or segmented nuclei (S), and kidney-shaped nuclei (K). Frequency of nuclear lesions were assessed totally for MN and all other lesions (L + S + K) and expressed per 1000 cells. At least 2000 cells were assessed for MN and nuclear lesions in each sample.

#### 2.4.3. Enzyme activities

Microsomal ethoxyresorufin-*O*-deethylase (EROD) activity was measured as a common and reliable indicator of the activity of the cytochrome P450 family I (CYP450 I) enzymes involved in Phase I biotransformation of xenobiotics in frog liver (Iwamoto et al., 2012). EROD was assayed in the microsomal fraction of the liver tissues. To obtain the microsomal fraction, postmitochondrial supernatant was obtained by centrifugation of the liver homogenates for 20 min at 12,000*g*, and the microsomal fraction was obtained by calcium (80 mM $CaCl_2$) precipitation of the postmitochondrial supernatant in 10 mM Tris-HCl buffer, pH 7.4 as described elsewhere (Cinti et al., 1972). EROD activity was

Please cite this article in press as: Falfushynska, H., et al. A calcium channel blocker nifedipine distorts the effects of nano-zinc oxide on metal metabolism in the marsh frog *Pelophylax ridibundus*. Saudi Journal of Biological Sciences (2017), https://doi.org/10.1016/j.sjbs.2017.10.004

detected by measuring the change in absorbance of resorufin at 572 nm (Klotz et al., 1984) and calculated using a molar extinction coefficient of 73.2 $mM^{-1}$ $cm^{-1}$ and standardized to the microsomal protein content.

The phenoloxidase-like activity of tyrosinase (EC 1.14.18.1) was determined by recording the formation of o-quinones (Luna-Acosta et al., 2011). p-Phenylenediamine were used as substrate. Phenoloxidase-like activity was monitored during 2 h at 420 nm. The amount of o-quinones was determined by using a molar extinction coefficient of 43 160 $M^{-1}cm^{-1}$. Data were expressed as nmol $min^{-1}$ $mg^{-1}$ protein.

Cholinesterase (ChE, EC 3.1.1.7) activity was determined in the brain as the acetylthiocholine-cleaving ChE activity at 25 °C according to the colorimetric method of Ellman et al. (1961). Cholinesterase activity in the frog brain measured in this study mostly represents activity of acetylcholine esterase. Butyrylcholinesterase which can also non-specifically cleave choline-based esters, is found in blood plasma and would not contribute significantly to the cholesterase activity in the perfused brain samples. Enzyme activity was calculated using a molar extinction coefficient of $13.6 \cdot 10^3$ $M^{-1} \cdot cm^{-1}$ and standardized to the soluble protein content.

### 2.5. Statistical analysis

The results are presented as means ± standard deviation (S.D.). Data were tested for normality and homogeneity of variance by using Kolmogorov-Smirnoff and Levene's tests, respectively. Whenever possible, data were normalized by Box-Cox common transforming method. One-way ANOVA was used to test the effect of experimental exposures, followed by post hoc procedures. Since data were not normally distributed (Lilliefors' test), non-parametric tests (Kruskall–Wallis ANOVA and Mann–Whitney U-test) were performed (significant at $p < .05$). For detection of correlation, the Pearson's correlation test was also used at 0.05 level of significance.

The classification tree was built using Classification and Regression Tree (CART) software on the basis of all determined biological characteristics. A CART tree is a binary decision tree that is built by splitting a node into two subsidiary nodes repetitively, beginning with the root node that contains the whole learning sample and predicts the value of a target based on the values of independent variables. All statistical calculations were performed with Statistica v 10.0 and Excel programs for Windows-2000.

## 3. Results

### 3.1. Metal content and binding

MTs level in the liver tissue and their Zn and Cu-binding ability were affected by all exposures with the most prominent changes in response to $Zn^{2+}$ exposures (with up to 2.5 increase compared to the control levels) (Fig. 1A, C, D). All Zn-containing treatments ($Zn^{2+}$, n-ZnO and n-ZnO + Nfd) induced an increase in the tissue MTs content, while exposure to Nfd alone suppressed the MT levels (Fig. 1A). Notably, metal exposures ($Zn^{2+}$ and n-ZnO) led to an increased binding of Zn and Cu to MTs (Fig. 1C and D). Nfd treatment alone or in combination with n-ZnO caused the decrease of Zn and Cu binding to MTs (Fig. 1C and D).

All Zn-containing treatments ($Zn^{2+}$, n-ZnO and n-ZnO + Nfd) led to an increase in the levels of Zn-binding Vtg-LP by 23.5–54.1% in the blood plasma of male frogs (Fig. 1B). Nfd alone had no effect plasma levels of Vtg-LP (Fig. 3).

### 3.2. Tissue redox status

Lactate concentrations in the liver tissues were slightly but significantly elevated by exposures to n-ZnO (alone or in the presence

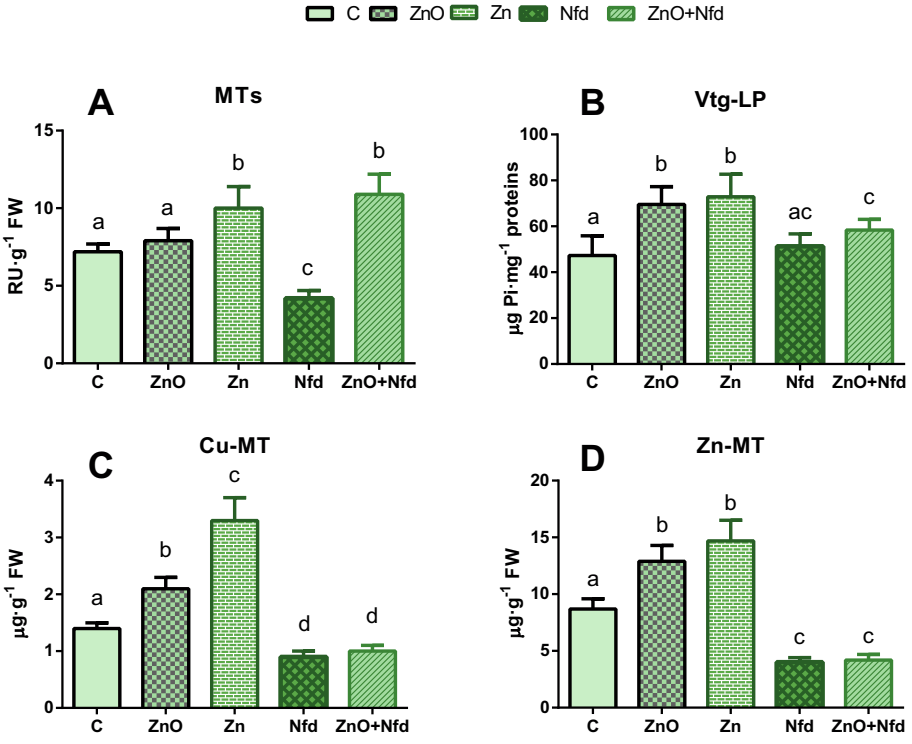


**Fig. 1.** Metallothioneins traits (A–D) and Zn-binding protein vitellogenin level (B) in frogs exposed to nano-zinc oxide (ZnO), zinc ions (Zn), nifedipine (Nfd) and combination of ZnO and Nfd. A: metallothioneins level, B: vitellogenin-like protein level, C: copper concentration in metallothioneins, D: zinc concentration in metallothioneins in the liver of frog *P. ridibundus*. Data are presented as means ± SD. N = 8 for MTs level and Vtg-LP and N = 3 (for joined samples from 5 specimens each) for Zn-MT, Cu-MT. Here and on the Figs. 2 and 3, the columns that share the same letters indicate the values that are not significantly different ($P > .05$).

Please cite this article in press as: Falfushynska, H., et al. A calcium channel blocker nifedipine distorts the effects of nano-zinc oxide on metal metabolism in the marsh frog *Pelophylax ridibundus*. Saudi Journal of Biological Sciences (2017), https://doi.org/10.1016/j.sjbs.2017.10.004

of Nfd) (Fig. 2A). Other treatments had no effect on tissue lactate levels. Pyruvate concentrations were suppressed by $Zn^{2+}$ and n-ZnO treatments and elevated in the presence of Nfd (Fig. 2B). As a result, lactate/pyruvate ratio increased in $Zn^{2+}$ and n-ZnO treatments and declined in Nfd-containing exposures (Fig. 2C).

PC levels in the liver tissues slightly but significantly increased after exposure to $Zn^{2+}$, and were considerably elevated after exposure to Nfd alone (Fig. 2D). In contrast, joint exposure to n-ZnO and Nfd led to a decrease in the protein carbonyl content in the frog liver (Fig. 2D).

### 3.3. Cellular stress and toxicity biomarkers

All experimental exposures resulted in elevated levels of nuclear abnormalities indicating genotoxicity (Fig. 3A). No neurocytotoxicity (assessed as ChE activity in the brain) was induced by the experimental exposures to $Zn^{2+}$ and n-ZnO + Nfd, while ChE activity was suppressed in n-ZnO exposed group (Fig. 3B). Notably, exposure to Nfd alone led to an increased activity of activation of ChE.

All experimental treatments (except n-ZnO) led to elevated activity of a Phase I biotransformation enzyme (EROD) in the liver (Fig. 3C). The tyrosinase-like activity was suppressed in Nfd- and n-ZnO- exposed groups but not in those co-exposed to n-ZnO and Nfg (Fig. 3D). Notably, $Zn^{2+}$ exposure caused a twofold increase in tyrosinase activity compared to the control (Fig. 3).

### 3.4. Data integration

Pearson correlation analysis showed that all parameters related to metal homeostasis (MT levels, Cu- and Zn-MTs, Vtg-LP) are strongly and positively correlated with each other and with the lactate/pyruvate ratio (Table 1). CART analysis generated a tree with 4 splits and 5 terminal nodes, and the overall classification accuracy of 95% (Fig. 4). Nfd-treated groups were distinguished from the rest primarily by the low Cu-MT content. Within the Nfd-containing treatment groups, n-ZnO + Nfd treated group differed from those treated with Nfd alone by higher MT content. Control group and n-ZnO-exposed groups were segregated by the lactate/pyruvate ratio (lower in n-ZnO group), and $Zn^{2+}$-exposed group was distinguished by elevated tyrosinase activity.

## 4. Discussion

Ca-channel blockers such as Nfd are expected to affect $Zn^{2+}$ metabolism due to the tight linkages between the metabolism and transport of $Ca^{2+}$ and $Zn^{2+}$ in the cell (Hogstrand et al., 1996, Nolte et al., 2004, Inoue et al., 2015). Thus, $Zn^{2+}$ can replace $Ca^{2+}$ in the binding sites of wide range of transport proteins such as the mitochondrial $Ca^{2+}$ transporter and the $Ca^{2+}$ channels located in excitable membranes (Csermely et al., 1989), and $Zn^{2+}$ blocks $Ca^{2+}$ entry through the same channels (Kerchner et al., 2000, Rogers and Wood, 2004). On the other hand, Zn uptake can be inhibited by Ca channel blockers Nfd, verapamil and lanthanum in some organisms, among them an euryhaline black sea bream (*Acanthopagrus schlegeli*) (Zhang and Wang, 2007) and a mangrove crab *Ucides cordatus* (Sá and Zanotto, 2013). Our present study is in line with these earlier findings showing that n-ZnO-induced elevation of Zn-MT levels is prevented by exposure to Nfd. Interestingly, Nfd exposure also suppressed levels of Cu-MT indicating that this Ca channel blocker may affect metabolism of several bivalent metals. One possible mechanism of Zn-MTs and Cu-MTs suppression may be related to Nfd-induced inhibition of the L-type voltage-gated Ca channel. Last one is responsible for the influx of zinc and copper ions and paracellular uptake route of these metals in *P. ridibundus* (Glover and Hogstrand, 2002).

MTs are the unique small cysteine-rich (up to 30%) cytosolic proteins which play a critical role in Zn and Cu buffering, transition

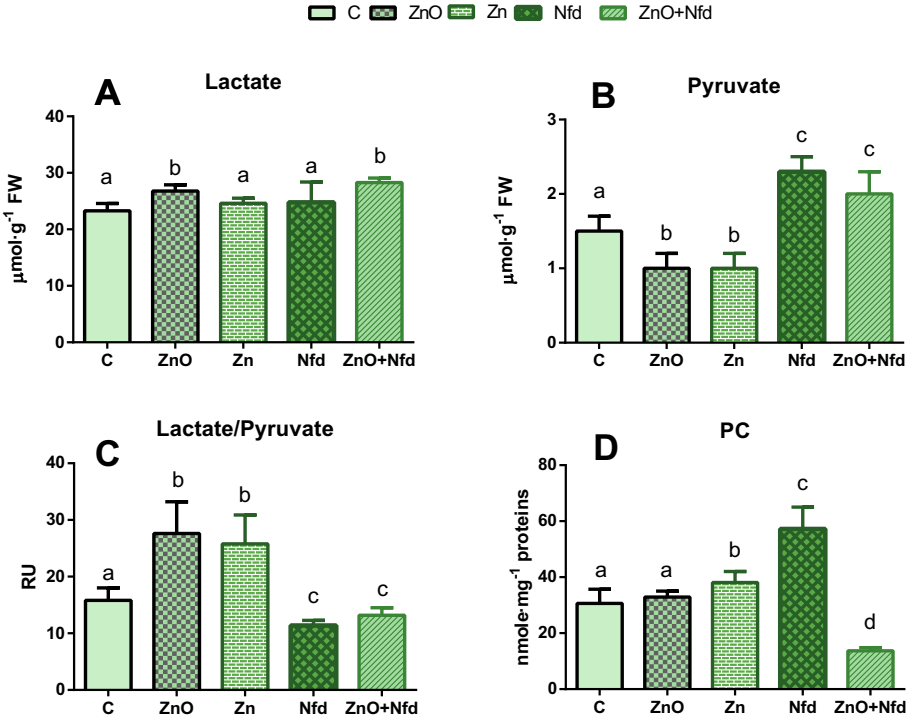


**Fig. 2.** Characteristics of metabolic activity, redox-state and stress marker in the liver of frog *P. ridibundus* exposed to nano-zinc oxide (ZnO), zinc ions (Zn), nifedipine (Nfd) and combine exposure. A: Lactate concentration, B: Pyruvate concentration C: Lactate to Pyruvate concentration ratio, D: protein carbonyls concentration. Data are presented as means ± SD (N = 8).

Please cite this article in press as: Falfushynska, H., et al. A calcium channel blocker nifedipine distorts the effects of nano-zinc oxide on metal metabolism in the marsh frog *Pelophylax ridibundus*. Saudi Journal of Biological Sciences (2017), https://doi.org/10.1016/j.sjbs.2017.10.004

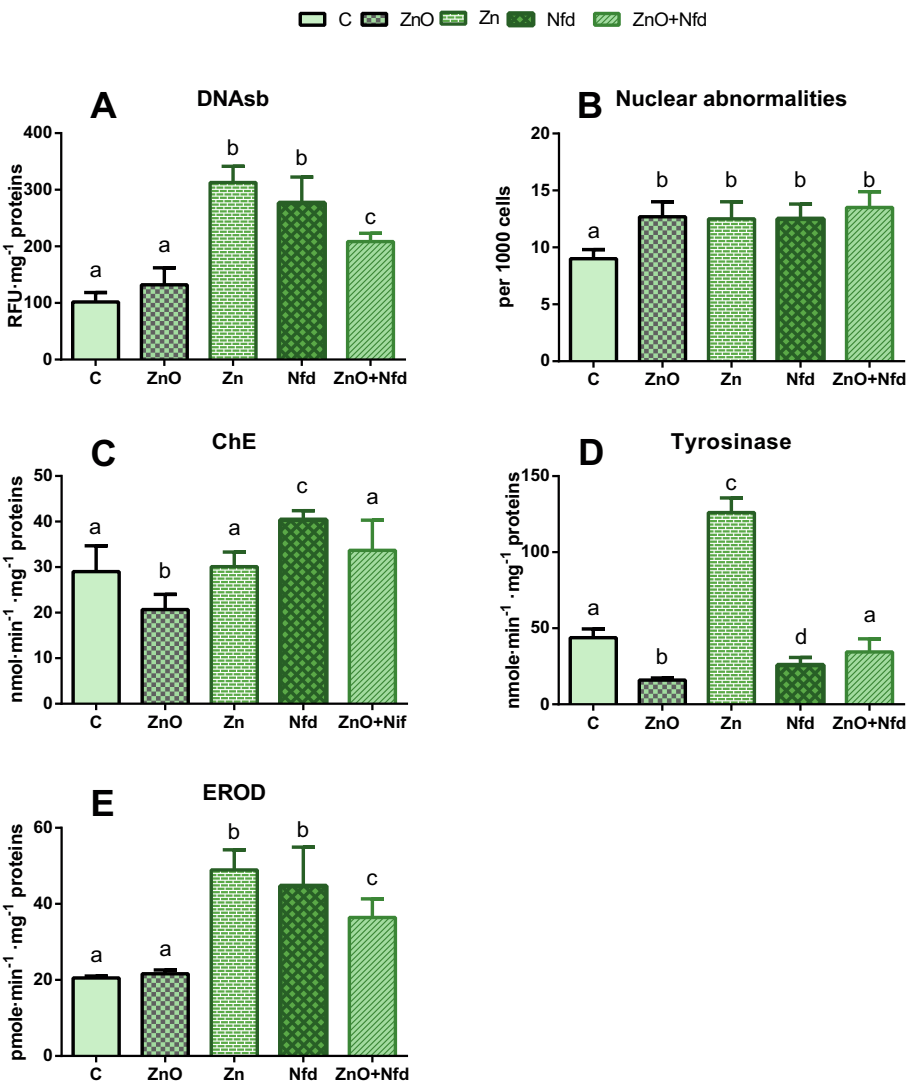


**Fig. 3.** Characteristics of genotoxicity, melanogenesis, neurotoxicity and xenobiotic detoxification in the liver (A, C–E) and blood (B) of frog *P. ridibundus* exposed to nano-zinc oxide (ZnO), zinc ions (Zn), nifedipine (Nfd) and combine exposure. A: DNA strand breaks; B: Nuclear abnormalities; C: Cholinesterase activity; D: Tyrosinase like activity; E: EROD activity. Data are presented as means ± SD (N = 8).

metals, preferentially cadmium and mercury, detoxification, scavenging of reactive oxygen species (Kagi and Schaffer, 1988, Isani and Carpenè, 2014, Kimura and Kambe, 2016). It has been proposed that MTs play an important role in Zn homeostasis by controlling cellular Zn uptake, distribution, storage, and release (Maret, 2011, Kimura and Kambe, 2016). Moreover, Zn can stimulate MTs synthesis (Suzuki et al., 1990). Despite Zn is a weaker inductor of MTs than cadmium (Onosaka et al., 1984), numerous investigations have reported that Zn should affect MTs concentration and their mRNA synthesis in various species, among them freshwater vertebrate. It has been shown that the muscle MT-A and MT-B genes were up-regulated in mature rainbow trout (*Oncorhynchus mykiss*) under Zn exposure (1 mg $L^{-1}$ $ZnSO_4.7H_2O$) during 6, 12, 24, and 48 h of treatment (Ceyhun et al., 2001). Moreover, $Zn^{2+}$ in concentration of 100 μg·caused elevation of the Zn-MTs in the frog (*P. ridibundus*) liver, but no changes were observer for total MTs concentration (Falfushynska et al., 2015b). However, the ability of nanosized Zn either in n-ZnO or synthetic polymeric complex to affect MTs induction has not been well understood yet. Some results proposed different assertions related to wide range of animals (different fila), which vary from MTs induction to their oppression. A rapid up-regulation of MTs mRNA by n-ZnO has been reported in the liver of Arbor Acres chickens (Xiao-bo et al., 2009), in the kidney of Wistar rats (Hejazy et al., 2014). In present work both Zn and n-ZnO provoked prominent changes in MTs-related traits in frog liver either concentration or metal-binding ability refer to Zn or Cu. Obviously the up-regulated expression of MTs should occur due to releasing free metal ions from the surface of the nanoparticles (Shaw and Handy, 2011). In agreement with abovementioned, Zn-containing exposures alone or in combination had slight or no effect on antioxidant system of frog liver, independently of the effect on DNA fragmentation. In contrast, products of oxidative damage, PC, and genotoxicity, fragmented DNA and frequency of nuclear abnormalities, were strongly increased after Nfd treatment. This event was happened with a simultaneously deep oppression of putative radical scavenger, MTs. Of interest, the scavenging capacity of MT2A towards free •OH and peroxyl radicals is found to be 100-fold higher than that of GSH (Lian et al., 2013).

It has been expected that Zn- and Nfd-containing exposures provoked opposite changes of lactate/pyruvate ratio in frog liver. Several studies give the evidence of Zn linkage to the glucose homeostasis (Jansen et al., 2009), but generally it was obtained with using mammals as a model. For instance, the addition of $ZnCl_2$

Please cite this article in press as: Falfushynska, H., et al. A calcium channel blocker nifedipine distorts the effects of nano-zinc oxide on metal metabolism in the marsh frog *Pelophylax ridibundus*. Saudi Journal of Biological Sciences (2017), https://doi.org/10.1016/j.sjbs.2017.10.004

**Table 1**
Relationships between the studied biological traits in the liver, brain and blood of *P. ridibundus* exposed to tap water (control), nano-zinc oxide, zinc ions, nifedipine and combine exposure to nano-zinc oxide and nifedipine.

| | Zn-MT | ChE | Lac/Pyr | DNAsb | Vtg-LP | Tyr-LA | MT | EROD | Cu-MT | NA | PC | Lac | Pyr |
|---|---|---|---|---|---|---|---|---|---|---|---|---|---|
| Zn-MT | | **−.6515 p = .000** | **.8839 p = .000** | −.0054 p = .974 | **.4500 p = .004** | **.5678 p = .000** | **.3813 p = .015** | −.0889 p = .586 | **.9313 p = .000** | −.0605 p = .711 | .0034 p = .983 | −.1895 p = .242 | **−.9146 p = .000** |
| ChE | | | **−.6709 p = .000** | **.5583 p = .000** | **−.8706 p = .000** | .0538 p = .742 | −.2204 p = .172 | **.5773 p = .000** | **−.4291 p = .006** | .0745 p = .648 | **.3864 p = .014** | .0020 p = .990 | **.7538 p = .000** |
| Lac/Pyr | | | | −.0450 p = .783 | **.5170 p = .001** | **.3417 p = .031** | **.3472 p = .028** | −.1441 p = .375 | **.7993 p = .000** | .1686 p = .298 | −.0282 p = .863 | .0889 p = .586 | **−.8944 p = .000** |
| DNAsb | | | | | **−.7631 p = .000** | **.5895 p = .000** | .1194 p = .463 | **.9443 p = .00** | **.3184 p = .045** | **.4922 p = .001** | **.4361 p = .005** | .0767 p = .638 | .1915 p = .237 |
| Vtg-LP | | | | | | **−.3693 p = .019** | .1616 p = .319 | **−.7777 p = .000** | .1471 p = .365 | −.1042 p = .522 | **−.4627 p = .003** | .1542 p = .342 | **−.5597 p = .000** |
| Tyr-LA | | | | | | | **.5578 p = .000** | **.5740 p = .000** | **.7934 p = .000** | −.0132 p = .936 | .0484 p = .767 | −.2561 p = .111 | **−.4242 p = .006** |
| MTs | | | | | | | | .1409 p = .386 | **.4880 p = .001** | .2060 p = .202 | **−.7103 p = .000** | **.3519 p = .026** | **−.3967 p = .011** |
| EROD | | | | | | | | | .2370 p = .141 | **.4510 p = .003** | **.3863 p = .014** | .1471 p = .365 | .2583 p = .108 |
| Cu-MT | | | | | | | | | | .1082 p = .506 | .0501 p = .759 | −.1801 p = .266 | **−.8030 p = .000** |
| NA | | | | | | | | | | | −.0754 p = .644 | **.5309 p = .000** | .1175 p = .470 |
| PC | | | | | | | | | | | | **−.2997** p = .060 | .1458 p = .369 |
| Lac | | | | | | | | | | | | | .0963 p = .554 |
| Pyr | | | | | | | | | | | | | |

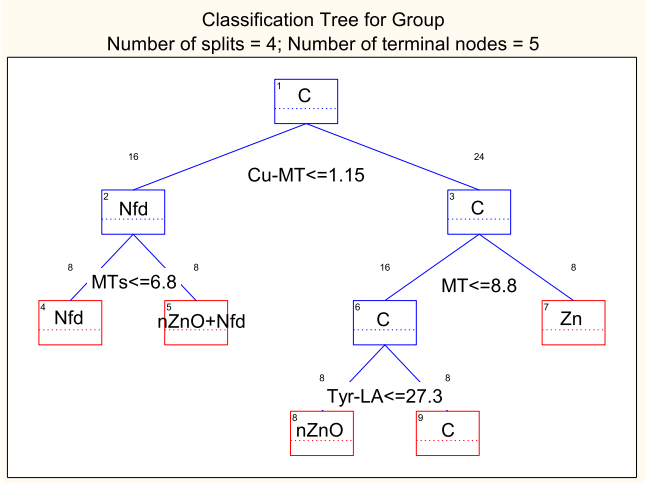


**Fig. 4.** Results of the classification and regression tree analysis of the studied biological traits of *P. ridibundus* from studied groups (C, nZnO, Zn, Nfd and nZnO + Nfd – frogs exposed to tap water (control), nano-zinc oxide, zinc ions, nifedipine and combine exposure to nano-zinc oxide and nifedipine respectively). The stepwise classification procedure identifies, at each step, a treatment group that is most different from all others based on the values of a certain biomarker. The distinguishing biomarker is shown near the branch split, and the group differentiated by that biomarker is shown in the corresponding terminal node. The lesser (<) sign next to the biomarker indicates that the value of the biomarker is greater in the terminal node group compared to all other groups. The number above each box indicates the number of animals in the respective group. Note that there was no misclassification of animals from any of the treatment groups, as N = 8 in each of the terminal nodes. Abbreviations: Cu-MT, copper concentration in metallothioneins, MTs, concentration of metallothioneins, Tyr-LA, tyrosinase like activity.

(20–80 μM) to the medium strongly stimulated lactate production and determined an increase in net glucose production in hepatocytes from fed rats (Brand and Kleineke, 1996). This effect is believed to be caused by elevation of intracellular Zn levels (Rofe et al., 2000). Treatment of cells with ZnO, but not $TiO_2$, depressed mitochondrial membrane potential, leading to a dose-dependent increase in glycogen breakdown by up to 430%, with an increase of both glycolysis and glucose release (Filippi et al., 2015). We have shown that increases of anaerobic processes and acidosis under Zn and n-ZnO were consistent with MTs level ($r = 0.35$, $p < .05$) and Zn-MT ($r = 0.88$, $p < .001$) in frog liver tissue. Indeed, stimulation of MTs synthesis may sufficiently reduce labile Zn in hepatocytes with subsequent stimulation of glycolysis via alteration of glycogen metabolism steps catalyzed by pyruvate kinase and by phosphofructokinase-1 (Brand and Kleineke, 1996). Thereby, Zn and its partitioning with MTs participation plays an important role in regulation of carbohydrate metabolism in frog organism.

The calcium channel blockers, when given either *in vivo* or *in vitro*, usually have marked decreased energy demands and both oppressed lactate dehydrogenase activity and lactate level. Several evidences of this phenomenon have been obtained mainly with using guinea pig hearts and rat hearts and muscles as a model (de Jong and Huizer, 1985, Becker and Möbert, 1999, Sato et al., 1999). However, our previous study with using bivalve mollusk *Unio tumidus* has shown significant lactate accumulation and a decrease in pyruvate levels after Nfd treatment, indicating transition to partial anaerobiosis and an increase in $NADH/NAD^+$ ratio (Falfushynska et al., 2015a). In present study lactate concentration in liver tissue didn't change, but Lac/Pyr was decreased after Nfd action alone and in combination with n-ZnO, and organism's response was closely related to higher vertebrate type. Obviously, Nfd exposure in frog liver caused suppression of calcium influx, preserves high-energy phosphates and exhibited ATP-saving effect.

Vtg, a Zn- and calcium-binding plasma protein, contains a total of 5 mol of metal/440 kDa dimer, 2 mol of Zn, and 3 mol of calcium in the *Xenopus laevis* and about 0.7% calcium, determined for the rainbow trout *Oncorhynchus mykiss* (Fremont and Riazi, 1988, Montorzi et al., 1995). Its high level in *P. ridibundus* seems to be

Please cite this article in press as: Falfushynska, H., et al. A calcium channel blocker nifedipine distorts the effects of nano-zinc oxide on metal metabolism in the marsh frog *Pelophylax ridibundus*. Saudi Journal of Biological Sciences (2017), https://doi.org/10.1016/j.sjbs.2017.10.004

dependent on Zn, both endo- and exogenous. We've shown that Vtg-LP level correlated with Zn-MTs ($r = 0.76$, $p < .001$), providing probably the sufficient supply of Zn in frog liver whenever Vtg synthesis occurs. On the other hand, moderate but significant activation of vitellogenesis was found in response to Zn, n-ZnO and n-ZnO + Nfd co-exposure. Moreover, Vtg-LP level in blood plasma was the primer marker for distinguishing of groups subjected to Zn-containing and Zn-free exposures according to CART analysis (Fig. 4). These data confirm the results obtained by alternative methods in the same model exposure (Falfushynska et al., 2017). There are several notes that Vtg level and/or expression is up-regulated as a response to estrogen-mimicking chemicals in male fish and amphibians (Palmer et al., 1998, Jones et al., 2000, Hutchinson et al., 2006). The up-regulation of Vtg-LP by exposures to Zn, Zn-containing nanomaterial and corresponding polymer substance based on vinylpirolidone was also found in frog *P. ridibundus* and fish *Carassius* sp. (Falfushynska et al., 2014, 2015b). Besides, in these studies Vtg-LP elevation was congruent in most cases with responses of tyrosinase-like and EROD activities.

Tyrosinase is a widespread indispensable binuclear Cu-enzyme that presents in the tissues of wide range of vertebrates, among them frog skin and liver pigment cells (Cicero et al., 1989). It takes part in melanogenesis and is able to protect cells *in vitro* against ROS-mediated toxicity (Rolff et al., 2011, Marino et al., 2011) and plays a crucial role in the innate immune (Pang et al., 2013). CART analysis has revealed tyrosinase-like activity as criterion of partitioning n-ZnO-treated animals (Fig. 4). There are several studies reported Zn-containing proteins or substances' caused inhibition either tyrosinase protein level or activity in a mixed-type inhibition manner (Hale, 2002, Han et al., 2007). However for n-ZnO such information has been unknown. Meanwhile, the same regularities we've observed in Nfd-treated animals. Some reports have declared calcium channel blockers depressing activity of immune competence cells *in vitro*. For example, it has shown Nfd- and verapamil-attenuated intracellular calcium levels, thereby inhibiting the proliferative *Plasmodium berghei*-specific T cell immune responses in Balb/C mice (Moshal et al., 2007). Moreover, they significantly suppressed both the sensitization and elicitation phases of a contact hypersensitivity reaction and functions of Langerhans cells (Katoh et al., 1997). Nfd and diltiazem inhibited proliferation of human whole blood lymphocyte cultures and formyl-methionyl-leucyl-phenylalanine-stimulated phagocytosis which is dependent on an increase in the concentration of $Ca^{2+}$ in human polymorphonuclear neutrophils (Rosales and Brown, 1992, Chow and Jusko, 2004). Our results allow predicting the immune disruptive effect of n-ZnO and Nfd for mature frog and the attenuation of immune system of wild animals promoting decline of amphibian population (Carey et al., 1999, Hayes et al., 2010).

In conclusion, this report presents results of complex study of the effects of n-ZnO in combination with widespread pharmaceutical Nfd using frog *P. ridibundus*. These data have further proved the bioavailability of Zn from n-ZnO in the organism of frog studied earlier, where the hypothesis was validated by thyrotropin-related parameters, lipofuscin accumulation, caspase-3 and CYP450 upregulation (Falfushynska et al., 2017). Present work gained our insights into frog's immunity, bioenergetics and biotransformation response when they are facing co-exposure to these widespread substances. We found that n-ZnO and Zn could interfere endocrine system, cause elevation of metal-binding ability of MTs (both Zn and Cu) and shifting to anaerobiosis in frog liver. Meanwhile Nfd alone and in co-exposure with n-ZnO oppresses metal-binding ability of MTs against Zn and Cu, showing an ability to promote oxidative lesions and cytotoxic changes. It is evident that the release of common pharmaceuticals and nanoparticles into the aquatic environment is a matter of concern for their combined toxicity.

## Acknowledgements

This work has been supported by the Ministry of Education and Science of Ukraine (Projects # 118B, 125B; 131B, research project of young scientist (ID 97507)), Fulbright Scholarship, Alexander von Humboldt Foundation and West-Ukrainian Biomedical Research Centre grant. The authors thank Inna Sokolova for her useful comments on an earlier version of this manuscript.

## References

Adamcakova-Dodd, A., Stebounova, L.V., Kim, J.S., Vorrink, S.U., Ault, A.P., O'Shaughnessy, P.T., Grassian, V.H., Thorne, P.S., 2014. Toxicity assessment of zinc oxide nanoparticles using sub-acute and sub-chronic murine inhalation models. Part. Fibre. Toxicol. 11, 1–15.

Baršienė, J., Andreikenaite, L., Rybakovas, A., 2006. Cytogenetic damage in perch (*Perca fluviatilis* L.) and duck mussel (*Anodonta anatina* L.) exposed to crude oil. Ekologija 1, 25–31.

Becker, B.F., Möbert, J., 1999. Low-dosecalcium antagonists reduce energy demand and cellular damage of isolated hearts during both ischemia and reperfusion. Naunyn Schmiedebergs Arch. Pharmacol. 360, 287–294.

Bester, M.J., Potgieter, H.C., Vermaak, W.J.H., 1994. Cholate and pH reduce interference by sodium dodecyl sulfate in the determination of DNA with Hoechst. Anal. Biochem. 223, 299–305.

Beukelman, T.E., Lord, S.S., 1960. The standard addition technique in flame spectrometry. Appl. Spectrosc. 14, 12–17.

Brand, I.A., Kleineke, J., 1996. Intracellular zinc movement and its effect on the carbohydrate metabolism of isolated rat hepatocytes. J. Biol. Chem. 271, 1941–1949.

Buzea, C., Pacheco, I.I., Robbie, K., 2007. Nanomaterials and nanoparticles: sources and toxicity. Biointerphases 2, MR17–MR71.

Carey, C., Cohen, N., Rollins-Smith, L., 1999. Amphibian declines: an immunological perspective. Dev. Comp. Immunol. 23, 459–472.

Ceyhun, S.B., Aksakal, E., Ekinci, D., Erdoğan, O., Beydemir, Ş., 2001. Influence of cobalt and zinc exposure on mRNA expression profiles of metallothionein and cytocrome P450 in rainbow trout. Biol. Trace. Elem. Res. 144, 781–789.

Chow, F.S., Jusko, W.J., 2004. Immunosuppressive interactions among calcium channel antagonists and selected corticosteroids and macrolides using human whole blood lymphocytes. Drug. Metab. Pharmacokinet. 19, 413–421.

Cicero, R., Mallardi, A., Maida, I., Gallone, A., Pintucci, G., 1989. Melanogenesis in the pigment cells of Rana esculenta L. liver: evidence for tyrosinase-like activity in the melanosome protein fraction. Pigment. Cell. Res. 2, 100–108.

Cinti, D.L., Moldeus, P., Schenkman, J.B., 1972. Kinetic parameters of drug metabolizing enzymes in Ca2+-sedimented microsomes from rat liver. Biochem. Pharmacol. 21, 3249–3256.

Csermely, P., Sándor, P., Radics, L., Somogyi, J., 1989. Zinc forms complexes with higher kinetical stability than calcium, 5-F-BAPTA as a good example. Biochem. Biophys. Res. Commun. 165, 838–844.

Daughton, C.G., 2016. Pharmaceuticals and the Environment (PiE): evolution and impact of the published literature revealed by bibliometric analysis. Sci. Total. Environ. 562, 391–426.

de Jong, J.W., Huizer, T., 1985. Reduced glycolysis by nisoldipine treatment of ischemic heart. J. Cardiovasc. Pharmacol. 7, 497–500.

Ellman, G.L., Courtney, K.D., Andres, V.J., Featherstone, R.M., 1961. A new and rapid colorimetric determination of acetylcholinesterase activity. Biochem. Pharmacol. 7, 88–95.

Falfushynska, H., Gnatyshyna, L., Fedoruk, O., Mitina, N., Zaichenko, A., Stoliar, O., Stoika, R., 2015a. Hepatic metallothioneins in molecular responses to cobalt, zinc, and their nanoscale polymeric composites in frog *Rana ridibunda*. Comp. Biochem. Physiol. C. Toxicol. Pharmacol. 172–173, 45–56.

Falfushynska, H., Gnatyshyna, L., Horyn, O., Sokolova, I., Stoliar, O., 2017. Endocrine and cellular stress effects of zinc oxide nanoparticles and nifedipine in marsh frogs *Pelophylax ridibundus*. Aquat. Toxicol. 185, 171–182.

Falfushynska, H., Gnatyshyna, L., Turta, O., Stoliar, O., Mitina, N., Zaichenko, A., Stoika, R., 2014. Responses of hepatic metallothioneins and apoptotic activity in *Carassius auratus gibelio* witness a release of cobalt and zinc from waterborne nanoscale composites. Comp. Biochem. Physiol. C 160, 66–74.

Falfushynska, H., Gnatyshyna, L., Yurchak, I., Sokolova, I., Stoliar, O., 2015b. The effects of zinc nanooxide on cellular stress responses of the freshwater mussels *Unio tumidus* are modulated by elevated temperature and organic pollutants. Aquat. Toxicol. 162, 82–93.

Falfushynska, H.I., Stoliar, O.B., 2009. Function of metallothioneins in carp *Cyprinus carpio* from two field sites in Western Ukraine. Ecotoxicol. Environ. Saf. 72, 1425–1432.

Filippi, C., Pryde, A., Cowan, P., Lee, T., Hayes, P., Donaldson, K., Plevris, J., Stone, V., 2015. Toxicology of ZnO and TiO2 nanoparticles on hepatocytes: impact on metabolism and bioenergetics. Nanotoxicology 9, 126–134.

Frasco, M.F., Fournier, D., Carvalho, F., Guilhermino, L., 2005. Do metals inhibit acetylcholinesterase (AChE)? Implementation of assay conditions for the use of AChE activity as a biomarker of metal toxicity. Biomarkers 10, 360–375.

Fremont, L., Riazi, A., 1988. Biochemical analysis of vitellogenin from rainbow trout (Salmo gairdneri): fatty acid composition of phospholipids. Reprod. Nutr. Dev. 28, 939–952.

Gawehn, K., 1988. D-(-)-Lactate. In: Bergmeyer, H.U. (Ed.), Methods of Enzymatic Analysis, third ed., vol. VI. VCH Publishers (UK) Ltd., Cambridge, UK, pp. 588–592.

Glover, C.N., Hogstrand, C., 2002. *In vivo* characterisation of intestinal zinc uptake in freshwater rainbow trout. J. Exp. Biol. 205, 141–150.

Hale, L.P., 2002. Zinc alpha-2-glycoprotein regulates melanin production by normal and malignant melanocytes. J. Invest. Dermatol. 119, 464–470.

Han, H.Y., Zou, H.C., Jeon, J.Y., Wang, Y.J., Xu, W.A., Yang, J.M., Park, Y.D., 2007. The inhibition kinetics and thermodynamic changes of tyrosinase via the zinc ion. Biochim. Biophys. Acta 1774, 822–827.

Hayase, N., Inagaki, S., Abiko, Y., 1995. Effects of photodegradation products of nifedipine: the nitroso-derivative relaxes contractions of the rat aortic strip induced by norepinephrine and other agonists. J. Pharmacol. Exp. Ther. 275, 813–821.

Hayes, T.B., Falso, P., Gallipeau, S., Stice, M., 2010. The cause of global amphibian declines: a developmental endocrinologist's perspective. J. Exp. Biol. 213, 921–933.

Hejazy, M., Koohi, M.K., Asadi, F., Behrouz, H.J., 2014. Induction of renal metallothionein expression by nano-zinc in cadmium-treated rats. Comp. Clin. Path. 23, 1477–1483.

Hogstrand, C., Verbost, P.M., Bonga, S.E., Wood, C.M., 1996. Mechanisms of zinc uptake in gills of freshwater rainbow trout: interplay with calcium transport. Am. J. Physiol. 270, R1141–R1147.

Hutchinson, T.H., Ankley, G.T., Segner, H., Tyler, C.R., 2006. Screening and testing for endocrine disruption in fish – biomarkers as "signposts", not "traffic lights", in risk assessment. Environ. Health. Perspect. 114, 106–114.

Inoue, K., O'Bryant, Z., Xiong, Z.G., 2015. Zinc-permeable ion channels: effects on intracellular zinc dynamics and potential physiological/pathophysiological significance. Curr. Med. Chem. 22, 1248–1257.

Isani, G., Carpenè, E., 2014. Metallothioneins, unconventional proteins from unconventional animals: a long journey from nematodes to mammals. Biomolecules 4, 435–457.

Iwamoto, D.V., Kurylo, C.M., Schorling, K.M., Powell, W.H., 2012. Induction of cytochrome P450 family 1 mRNAs and activities in a cell line from the frog *Xenopus laevis*. Aquat. Toxicol. 114–115, 165–172.

Jansen, J., Karges, W., Rink, L., 2009. Zinc and diabetes–clinical links and molecular mechanisms. J. Nutr. Biochem. 20, 399–417.

Johnson, M.S., Aubee, C., Salice, C.J., Leigh, K.B., Liu, E., Pott, U., Pillard, D., 2016. A review of ecological risk assessment methods for amphibians: comparative assessment of testing methodologies and available data. Integr. Environ. Assess. Manag. 9999, 1–13.

Jones, P.D., De Coen, W.M., Tremblay, L., Glesy, J.P., 2000. Vitellogenin as a biomarker for environmental estrogens. Water Sci. Technol. 42, 1–14.

Kagi, J.H.R., Schaffer, A., 1988. Biochemistry of metallothionein. Biochemistry 27, 8509–8515.

Katoh, N., Hirano, S., Kishimoto, S., Yasuno, H., 1997. Calcium channel blockers suppress the contact hypersensitivity reaction (CHR) by inhibiting antigen transport and presentation by epidermal Langerhans cells in mice. Clin. Exp. Immun. 108, 302–308.

Kerchner, G.A., Canzoniero, L.M.T., Yu, S.P., Ling, C., Choi, D.W., 2000. $Zn^{2+}$ current is mediated by voltage-gated $Ca^{2+}$ channels and enhanced by extracellular acidity in mouse cortical neurones. J. Physiol. 528, 39–52.

Kim, R.O., Choi, J.S., Kim, B.C., Kim, W.K., 2017. Comparative analysis of transcriptional profile changes in larval zebrafish exposed to zinc oxide nanoparticles and zinc sulfate. Bull. Environ. Contam. Toxicol. 98, 183–189.

Kimura, T., Kambe, T., 2016. The functions of metallothionein and ZIP and ZnT transporters: an overview and perspective. Int. J. Mol. Sci. 17, 336.

Kloas, W., Lutz, I., 2006. Amphibians as model to study endocrine disrupters. J. Chromatogr. A 1130, 16–27.

Klotz, A.V., Stegeman, J.J., Walsh, C., 1984. An alternative 7-ethoxyresorufin O-deethylase activity assay: a continuous visible spectrophotometric method for measurement of cytochrome P-450 monooxygenase activity. Anal. Biochem. 140, 138–145.

Lamprecht, W., Heinz, F., 1988. Pyruvate, in: Bergmeyer, H.U. (Ed.), Methods of Enzymatic Analysis, third ed., vol. VI. VCH Publishers (UK) Ltd., Cambridge, UK, pp. 570–577.

Lian, Y., Zhao, J., Xu, P., Wang, Y., Zhao, J., Jia, L., Fu, Z., Jing, L., Liu, G., Peng, S., 2013. Protective effects of metallothionein on isoniazid and rifampicin-induced hepatotoxicity in mice. PLoS One 8, e72058.

Liu, J., Feng, X., Wei, L., Chen, L., Song, B., Shao, L., 2016. The toxicology of ion-shedding zinc oxide nanoparticles. Crit. Rev. Toxicol. 46, 348–384.

Lowry, O.H., Rosebroungh, H.J., Farr, A.L., Randall, R.J., 1951. Protein measurement with folin phenol reagent. J. Biol. Chem. 191, 265–275.

Luna-Acosta, A., Thomas-Guyon, H., Amari, M., Rosenfeld, E., Bustamante, P., Fruitier-Arnaudin, I., 2011. Differential tissue distribution and specificity of phenoloxidases from the Pacific oyster *Crassostrea gigas*. Comp. Biochem. Physiol. B. Biochem. Mol. Biol. 159, 220–226.

Maret, W.J., 2011. Redox biochemistry of mammalian metallothioneins. J. Biol. Inorg. Chem. 16, 1079–1086.

Marino, S.M., Fogal, S., Bisaglia, M., Moro, S., Scartabelli, G., De Gioia, L., Spada, A., Monzani, E., Casella, L., Mammi, S., Bubacco, L., 2011. Investigation of Streptomyces antibioticus tyrosinase reactivity toward chlorophenols. Arch. Biochem. Biophys. 505, 67–74.

Montorzi, M., Falchuk, K.H., Vallee, B.L., 1995. Vitellogenin and lipovitellin: zinc proteins of *Xenopus laevis* oocytes. Biochemistry 34, 10851–10858.

Moshal, K.S., Adhikari, J.S., Bist, K., Nair, U., Dwarakanath, B.S., Katyal, A., Chandra, R., 2007. Calcium channel antagonist (nifedipine) attenuates Plasmodium berghei-specific T cell immune responses in Balb/C mice. APMIS 115, 911–920.

Mulware, S.J., 2013. Trace elements and carcinogenicity: a subject in review. 3 Biotech 3, 85–96.

Nagler, J.J., Ruby, S.M., Idler, D.R., So, Y.P., 1987. Serum phosphoprotein phosphorus and calcium levels as reproductive indicators of vitellogenin in highly vitellogenic mature female and estradiol-injected immature rainbow trout (*Salmo gairdneri*). Can. J. Zool. 65, 2421–2425.

Nations, S., Long, M., Wages, M., Canas, J., Maul, J.D., Theodorakis, C., Cobb, G.P., 2011. Effects of ZnO nanomaterials on *Xenopus laevis* growth and development. Ecotoxicol. Environ. Saf. 74, 203–210.

Nolte, C., Gore, A., Sekler, I., Kresse, W., Hershfinkel, M., Hoffmann, A., Kettenmann, H., Moran, A., 2004. ZnT-1 expression in astroglial cells protects against zinc toxicity and slows the accumulation of intracellular zinc. Glia 48, 145–155.

Olive, P.L., 1988. DNA precipitation assay: a rapid and simple method for detecting DNA damage in mammalian cells. Environ. Molec. Mutagen. 11, 487–495.

Onosaka, S., Tanaka, K., Cheriant, M.G., 1984. Effects of cadmium and zinc on tissue levels of metallothionein. Environ. Health. Perspect. 54, 67–72.

Osmond, M.J., McCall, M.J., 2010. Zinc oxide nanoparticles in modern sunscreens: an analysis of potential exposure and hazard. Nanotoxicology 4, 15–41.

Palmer, B.D., Huth, L.K., Pieto, D.L., Selcer, K.W., 1998. Vitellogenin as a biomarker for xenobiotic estrogens in an amphibian model system. Environ. Toxicol. Chem. 17, 30–36.

Pandurangan, M., Kim, D.H., 2015. ZnO nanoparticles augment ALT, AST, ALP and LDH expressions in C2C12 cells. Saudi J. Biol. Sci. 22, 679–684.

Pang, Q., Liu, X., Sun, H., Zhang, S., Song, X., Zhang, X., Zhang, M., Bai, Y., Gao, L., Zhao, B., 2013. Cloning, characterization and expression of tyrosinase-like gene in amphioxus *Branchiostoma japonicum*. Fish. Shellfish. Immunol. 34, 356–364.

Pohanka, M., 2014. Copper, aluminum, iron and calcium inhibit human acetylcholinesterase in vitro. Environ. Toxicol. Pharmacol. 37, 455–459.

Prokić, M., Borković-Mitić, S., Krizmanić, I., Gavrić, J., Despotović, S., Gavrilović, B., Radovanović, T., Pavlović, S., Saičić, Z., 2017. Comparative study of oxidative stress parameters and acetylcholinesterase activity in the liver of *Pelophylax esculentus* complex frogs. Saudi J. Biol. Sci. 24, 51–58.

Reznick, A.Z., Packer, L., 1994. Oxidative damage to proteins: spectrophotometric method for carbonyl assay. Methods Enzymol. 233, 357–363.

Rofe, A.M., Philcox, J.C., Coyle, P., 2000. Activation of glycolysis by zinc is diminished in hepatocytes from metallothionein null mice. Biol. Trace. Elem. Res. 75, 87–97.

Rogers, J.T., Wood, C.M., 2004. Characterization of branchial lead-calcium interaction in the freshwater rainbow trout *Oncorhynchus mykis*. J. Exp. Biol. 207, 813–825.

Rolff, M., Schottenheim, J., Decker, H., Tuczek, F., 2011. Copper-O2 reactivity of tyrosinase models towards external monophenolic substrates: molecular mechanism and comparison with the enzyme. Chem. Soc. Rev. 40, 4077–4098.

Rosales, C., Brown, E.J., 1992. Calcium channel blockers nifedipine and diltiazem inhibit Ca2+ release from intracellular stores in neutrophils. J. Biol. Chem. 267, 1443–1448.

Sá, M.G., Zanotto, F.P., 2013. Characterization of copper transport in gill cells of a mangrove crab *Ucides cordatus*. Aquat. Toxicol. 144–145, 275–283.

Sato, R., Yamazaki, J., Nagao, T., 1999. Temporal differences in actions of calcium channel blockers on K+ accumulation, cardiac function, and high-energy phosphate levels in ischemic guinea pig hearts. J. Pharmacol. Exp. Ther. 289, 831–839.

Shaw, B.J., Handy, R.D., 2011. Physiological effects of nanoparticles on fish: a comparison of nanometals versus metal ions. Environ. Int. 37, 1083–1097.

Sirelkhatim, A., Mahmud, S., Seeni, A., Kaus, N.H.M., Ann, L.K., Bakhori, S.K.M., Hasan, H., Mohamad, D., 2015. Review on zinc oxide nanoparticles: antibacterial activity and toxicity mechanism. Nano-Micro Lett. 7, 219–242.

Sun, F., Dai, C., Xie, J., Hu, X., 2012. Biochemical issues in estimation of cytosolic free NAD/NADH ratio. PLoS One 7, e34525.

Suzuki, C.A., Ohta, H., Albores, A., Koropatnick, J., Cherian, M.G., 1990. Induction of metallothionein synthesis by zinc in cadmium pretreated rats. Toxicology 63, 273–284.

The Project of Emerging Nanotechnologies. Consumer Products Inventory: An Inventory of Nanotechnology-Based Consumer Products Introduced on the Market, 2013. <http://www.nanotechproject.org/> (accessed 23.02.15).

Vance, M.E., Kuiken, T., Vejerano, E.P., McGinnis, S.P., Hochella Jr., M.F., Rejeski, D., Hull, M.S., 2015. Nanotechnology in the real world: redeveloping the nanomaterial consumer products inventory. Beilstein J. Nanotechnol. 6, 1769–1780.

Vandebriel, R.J., De Jong, W.H., 2012. A review of mammalian toxicity of ZnO nanoparticles. Nanotechnol. Sci. Appl. 15, 61–71.

World Health Organization (WHO), 2015. WHO Model List of Essential Medicines, 19th List. <http://www.who.int/medicines/publications/essentialmedicines/en/> (accessed 04.15).

Xiao-bo, D., Li-xin, W., Hui, Y., 2009. Effect of nano-zinc oxide on liver metallothionein of AA chicken. Chinese J. Vet. Sci. 29 (2), 242–244.

Zhang, L., Wang, W.X., 2007. Waterborne cadmium and zinc uptake in a euryhaline teleost *Acanthopagrus schlegeli* acclimated to different salinities. Aquat. Toxicol. 84, 173–181.

Please cite this article in press as: Falfushynska, H., et al. A calcium channel blocker nifedipine distorts the effects of nano-zinc oxide on metal metabolism in the marsh frog *Pelophylax ridibundus*. Saudi Journal of Biological Sciences (2017), https://doi.org/10.1016/j.sjbs.2017.10.004